

## Synthesis, structural characterization, electric and magnetic behaviour of a $\text{Sr}_2\text{DyNbO}_6$ double Perovskite

P.C. Plazas Hurtado<sup>1</sup>, D.A. Landínez Téllez<sup>1</sup>, J.A. Cardona Vásquez<sup>1</sup>, C. A. Parra Vargas<sup>2</sup>, J. Roa-Rojas<sup>1</sup>

<sup>1</sup> Grupo de Física de Nuevos Materiales, Departamento de Física, Universidad Nacional de Colombia, AA 5997, Bogotá DC, Colombia

<sup>2</sup> Grupo Física de Materiales, Escuela de Física, Universidad Pedagógica y Tecnológica de Colombia, Tunja, Colombia

E-mail: pcplazash@unal.edu.co

**Abstract.** Many multifunctional properties have been the focus of our interest in Perovskite research. Herein, we report synthesis and characterization of a new  $\text{Sr}_2\text{DyNbO}_6$  Perovskite-like material. Samples were produced via standard solid-state reaction method. Rietveld refinement of X-ray diffraction experimental data through the GSAS code reveals that this material crystallizes in a monoclinic complex Perovskite (space group  $P2_1/n$ , #14) with lattice parameters  $a=5.730(3)$  Å,  $b=5.905(1)$  Å and  $c=8.221(0)$  Å. Scanning electron microscopy images reveal that samples evidence a surface with strongly diffuse granular structure. From curves of magnetization as a function of temperature, we determined the paramagnetic behaviour of this complex Perovskite in the temperature regime between 50 and 320 K. Curie fitting allows obtaining an effective magnetic moment of  $10.28 \mu_B$ . Polarization curves as a function of the applied electric field show a hysteretic behavior of typical dielectric loss with relative dielectric constant of 264.28 at room temperature.

**Keywords:** Complex Perovskite, structure, magnetic behaviour

### Introduction

In recent years, much interest has emerged in electronic oxide ceramic oxides with  $\text{ABO}_3$  Perovskite structure due to their chemical versatility to evaluate different combinations of transition metal cation in the B site and obtain a variety of magnetic and electric properties [1]. Ideally, a simple  $\text{ABO}_3$  Perovskite possesses a tri-dimensional cubic network of  $\text{BO}_6$  octahedra with the cation A into the void formed by eight octahedra with  $\text{AO}_{12}$  coordination [2]. If the A and B sites contain a mixture of cations, distorted complex Perovskite structures with lower symmetries are obtained. Distortions are mainly related to octahedral tilting due to small cation driving a rotating of octahedra with respect to the crystallographic axes. Another kind of distortion is the cation displacement caused through first- and second-order Jahn-Teller effects. Specially, the 1:1 B-site based class with chemical formula  $\text{A}_2\text{BB}'\text{O}_6$  (or double Perovskites) is the most frequently encountered complex Perovskite [3]. From the distortions and composition of the double Perovskites, new properties and applications are found in ferroelectric devices with large dielectric constants and frequency dispersion [4], multiferroicity [5], solar energy conversion [6], catalysis [7], solid-oxide fuel cells [8], and microwave resonator [9]. Previous studies have shown that under certain conditions, the double Perovskite  $\text{Sr}_2\text{RESbO}_6$  (RE=Dy,



Ho, Gd) crystallizes in geometrically frustrating fcc lattices [10]. In this study, the authors report that the  $RE^{3+}$  and  $Sb^{5+}$  cations adopt an ordered array in the double-Perovskite structure with alternate octahedra. For  $RE=Dy$ , frustrated magnetic ordering has been observed. In order to study the effect of the substitution of  $Nb^{5+}$  in the crystallographic site of the  $Sb^{5+}$  on the crystal structure and magnetism, we synthesize the non-studied  $Sr_2DyNbO_6$  double Perovskite. On the other hand, due to the paramagnetic insulator behaviour reported at room temperature for the  $Sr_2RESbO_6$  [10], the electric polarizability of this material is particularly interesting.

### Experimental

Samples were synthesized by means of the standard solid-state reaction recipe. The precursor powders  $SrCO_3$ ,  $Dy_2O_3$ , and  $Nb_2O_5$  (Aldrich 99.9%) were stoichiometrically mixed according to the chemical formula  $Sr_2DyNbO_6$ . The mixture was annealed at 900 °C for 12 h. The samples were then reground, re-pelletized, and sintered at 1350 °C for 36 h. X-ray diffraction (XRD) experiments were performed by means of a PW1710 diffractometer with  $\lambda_{CuK\alpha}=1.54064\text{\AA}$ . Rietveld refinement of the diffraction pattern was made by the GSAS code [11]. Field cooling measurement of magnetization as a function of temperature was carried out by using VersaLab Quantum Design equipment. Morphological studies were performed via scanning electron microscopy (SEM) experiments through the utilization of a FEI Quanta 200 microscope. Polarization curves as a function of the applied electric field were obtained through a Radiant ferroelectric tester on the application of voltages up to 1000 V.

### Results and discussion

Figure 1 shows the XRD pattern for the  $Sr_2DyNbO_6$  double Perovskite at room temperature. It is clear from Figure 1 that the sample has a single crystallographic phase. From the Rietveld [11] it was determined that  $Sr_2DyNbO_6$  crystallizes in a monoclinic structure, space group  $P2_1/n$  (#14), which denotes a primitive cell with two-order screw axis ( $180^\circ$ ) rotation, followed by a translation of half lattice parameter in the [010] direction, and a glide plane reflection perpendicular to the [010] direction. The structure obtained is shown in Figure 2. The lattice parameters obtained were  $a = 5.7303 \text{ \AA}$ ,  $b = 5.9051 \text{ \AA}$ , and  $c = 8.2210 \text{ \AA}$ . The presence of the (211), (3-10), and (133) peaks in the diffraction pattern is an evidence of the possible cationic order of  $Dy^{3+}$  and  $Nb^{5+}$  in B and B' sites, respectively, of the  $A_2BB'O_6$  double Perovskite.

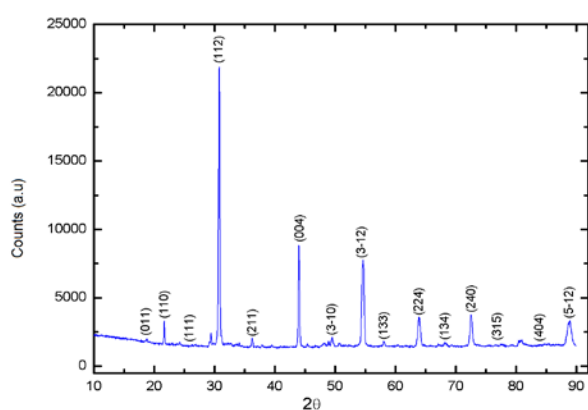


**Figure 1.** XRD pattern for the  $Sr_2DyNbO_6$  complex Perovskite

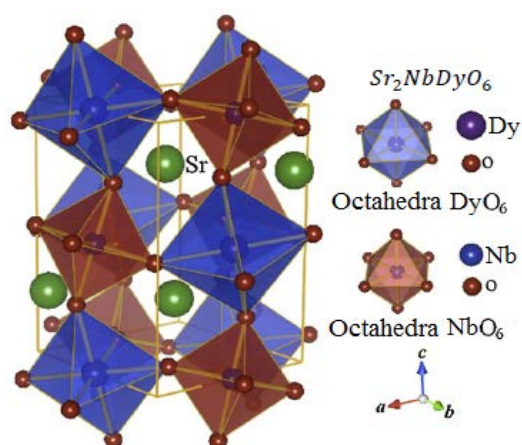


**Figure 2.** Crystalline structure of the  $Sr_2DyNbO_6$  double Perovskite

Figure 3 exemplifies the surface morphology of the  $\text{Sr}_2\text{DyNbO}_6$  sample. The SEM image shows homogeneous granularity, conformed by strongly diffused grains whose size varies from submicrometric up to micrometric scale ( $\sim 3 \mu\text{m}$ ).

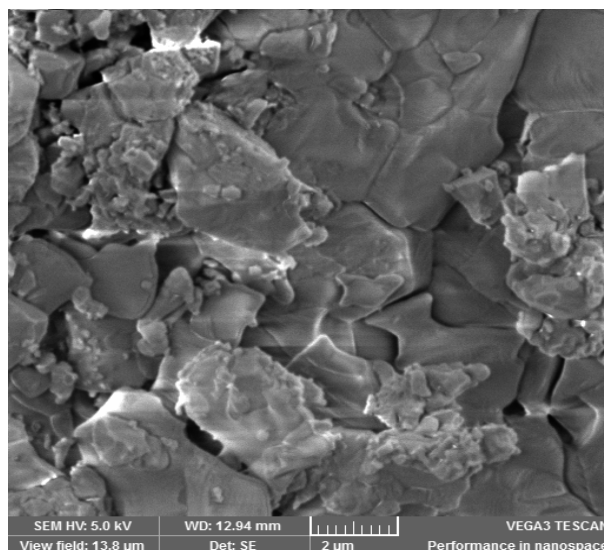


**Figure 3.** SEM image of the surface structure for the  $\text{Sr}_2\text{DyNbO}_6$  sample

Measurements of magnetic susceptibility as a function of temperature on the application of  $H = 10 \text{ Oe}$  reveals the paramagnetic behaviour of this material in the temperature regime from 50 to 300 K (results are shown in Figure 4).

From the fit of the susceptibility curve with the Curie behaviour given by  $\chi = C_c/T$ , we obtain a Curie constant  $C_c = 13.2423 \text{ emu}\cdot\text{K}/\text{mol}$ , which corresponds to an effective magnetic moment of  $\mu_{\text{eff}} = 10.28 \mu_B$ . This value agrees with the expected value of  $\mu_{\text{eff}} = 10.63 \mu_B$  predicted by Hund's rules for the isolated  $\text{Dy}^{3+}$  cation [12]. Figure 5 shows the hysteric behaviour of the electric polarization on the application of electric fields up to  $3.0 \text{ kV}/\text{cm}$ . The characteristic curve reveals strong dielectric loss with a saturation polarization of  $0.065 \mu\text{C}/\text{cm}^2$ , remnant polarization of  $0.039 \mu\text{C}/\text{cm}^2$  and coercive field of  $1.48 \text{ kV}/\text{cm}$ . From the estimated values of  $P_s$ , we determined the capacitance of the  $\text{Sr}_2\text{DyNbO}_6$  material through the equation  $P_s = (C/A)V$ , where  $A$  represents the area of the sample,  $V$  is the applied voltage, and  $C$  is the capacitance. Then, we obtained  $C/A$  by taking into account the range of high applied field of Figure 5 curve. The dielectric constant is calculated by the expression  $\varepsilon = (C/A)(d/\varepsilon_0)$ , where  $d$  represents the distance between the capacitor plates and  $\varepsilon_0$  is the dielectric constant in vacuum [13]. The value obtained of the relative dielectric constant at room temperature for the SZMO complex Perovskite is  $\varepsilon = 264.28$ , which is five times the value reported for  $\text{BaZrO}_3$  [14].

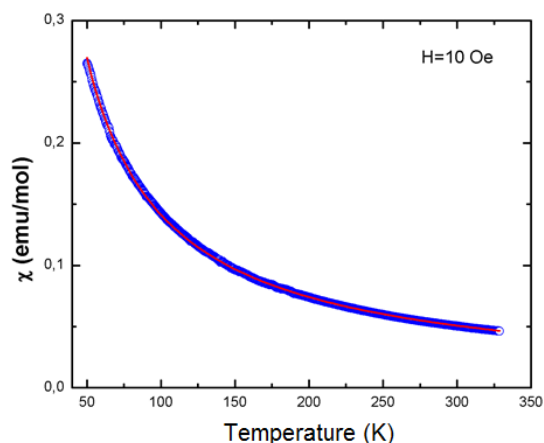


**Figure 4.** Curve of susceptibility as a function of temperature for the Sr<sub>2</sub>DyNbO<sub>6</sub> perovskite

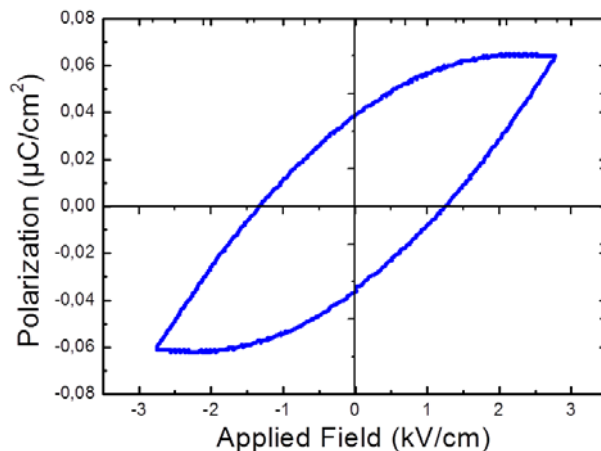


**Figure 5.** Hysteretic feature of the electric polarization for the Sr<sub>2</sub>DyNbO<sub>6</sub> Perovskite

### Conclusions

Synthesis and structural characterization of the new Sr<sub>2</sub>DyNbO<sub>6</sub> Perovskite-like material were performed. Rietveld analysis of experimental diffraction pattern reveals that this material crystallizes in a monoclinic complex Perovskite, which belongs to the space group P2<sub>1</sub>/n (#14). The SEM images reveal the strongly diffuse granular surface morphology. Measurements of magnetic susceptibility show the paramagnetic behaviour of the material in the temperature interval between 50 and 300 K. The experimental effective magnetic moment agrees with the theoretical value expected for the isolated Dy<sup>3+</sup> ion. The saturation of polarization in the dielectric hysteresis curve permitted determining the relative dielectric constant at room temperature  $\epsilon=264.28$ , which is an appropriate value for microwave applications.

### Acknowledgements

This work was partially supported by the Research Division (DIB) at Universidad Nacional de Colombia and “El Patrimonio Autónomo Fondo Nacional de Financiamiento para la Ciencia, la Tecnología y la Innovación Francisco, José de Caldas” – COLCIENCIAS, contract RC-No. 0850-2012.

### References

- [1] C. Franchini, 2014, J. Phys. Condens. Matter **26**, 253202.
- [2] L.C. Moreno, J.S. Valencia, D.A. Landínez Téllez, J. Arbey Rodríguez M., M.L. Martínez, J. Roa-Rojas, F. Fajardo, 2008, J. Magn. Magn. Mater. **320**, e19-e21.
- [3] C. J. Howard, B. J. Kennedy, P. M. Woodward, 2003, Acta Cryst. **B59**, 463-471.
- [4] E. J. Juárez-Perez, R. S. Sanchez, L. Badia, G. Garcia-Belmonte, Y. S. Kang, I. Mora-Sero, J. Bisquert, 2014, J. Phys. Chem. Lett. **5**, 2390-2394.
- [5] J. Roa-Rojas, C. Salazar M., D. Llamasa P., A.A. León-Vanegas, D.A. Landínez Téllez, P. Pureur, F.T. Dias, V.N. Vieira, 2008, J. Magn. Magn. Mater. **320**, e104-e106.
- [6] H.W. Eng, P.W. Barnes, B.M. Auer, P.M. Woodward, 2003, J. Solid State Chem. **175**, 94-109.
- [7] J. Suntivich, K.J. May, H.A. Gasteiger, J.B. Goodenough, Y. Shao-Horn, 2011, Science **334**, 1383-1385.
- [8] Y.-H. Huang, R.I. Dass, Z.-L. Xing, Z.-L. Xing, J.B. Goodenough, 2006, Science **312**, 254-257.
- [9] H.-L. Liu, H.-C. Hsueh, I.-N. Lin, M.-T. Yang, W.-C. Lee, Y.-C. Chen, C.-T. Chia, H.-F. Cheng, 2011, J. Phys.: Condens. Matter **23**, 225901.

- [10] H. Karunadasa, Q. Huang, B.G. Ueland, P. Schiffer, R.J. Cava, 2003, Proc. Natl. Acad. Sci. USA, **100**, 8097-80102.
- [11] A.C. Larson, R.B. Von Dreele, General Structure Analysis System, Los Alamos National Laboratory Report LAUR, 2000, 86.
- [12] Kittel, C., "*Introduction to Solid State Physics*", 8<sup>th</sup> Ed. University of California, Berkeley 2005.
- [13] D.A. Landínez Téllez, D. Llamasa P., C.E. Deluque Toro, Arles V. Gil Rebaza, J. Roa-Rojas, J., 2013, Mol. Struct. **1034**, 233-237.
- [14] G. Łupina, J. Dąbrowski, P. Dudek, G. Kozłowski, P. Zaumseil, G. Lippert, O. Fursenko, J. Bauer, C. Baristiran, I. Costina, H.-J. Müssig, L. Oberbeck, U. Schröder, 2009, Appl. Phys. Lett. **94**, 152903.